JOURNAL OF CATALYSIS 76, 369–384 (1982)

Sulfur Deactivation of Nickel Methanation Catalysts

W. D. FITZHARRIS,[1] J. R. KATZER,[2] AND W. H. MANOGUE[3]

Department of Chemical Engineering, University of Delaware, Newark, Delaware 19711

Received October 7, 1981; revised January 6, 1982

Sulfur deactivation of supported Ni in CO hydrogenation was studied in an all-quartz internal-recycle reactor with a feed containing 4% CO in H_2. Thirteen ppb H_2S reduced the steady-state methanation activity of Ni/γ-Al_2O_3 about 200-fold at 661 K; 100 ppb H_2S reduced the activity 5000-fold. A dual site Langmuir–Hinshelwood rate expression predicts both the CO partial pressure dependence and the S poisoning. Poisoning and chemisorption data indicate formation of a stable two-dimensional, surface sulfide with a S : Ni surface atom ratio of 1 : 2 for 13 ppb H_2S in H_2 at 661 K. The surface sulfide has a free energy of formation of at least −26 kcal/mole which is 15 kcal/mole more stable than bulk Ni_2S_3. Sulfur poisoning is due to geometric effects, i.e., site blockage, rather than electronic effects since the activation energy for methanation over S-poisoned Ni was the same as that over unpoisoned Ni, 24 kcal/mole.

INTRODUCTION

The conversion of synthesis gas (CO + H_2) produced by gasification of coal or other organic matter into high-quality fuels and chemicals is catalyzed by supported transition metals, which are very sensitive to the low concentrations of S-containing compounds which are inevitably present in the feed. For example, in the presence of gas streams containing 1 ppm H_2S, Ni and Co catalysts for methanation and Fischer–Tropsch are progressively poisoned until replacement of the catalyst becomes necessary, placing an undesirable burden on the process economics. Regeneration of S-poisoned Ni catalysts has not been successfully demonstrated (*1–3*) and, therefore, catalysts which maintain acceptable activity in the presence of moderate concentrations of S-containing gases are needed.

Few quantitative data are available on S deactivation of Ni catalysts. Losses of methanation activity from 100- to 1000-fold have been reported at S concentrations of 1 to 10 ppm H_2S (*4–7*), indicating the extreme sensitivity of Ni to S. The effect of S on the methanation rate was found to be nonlinear over Ni on magnesium aluminum spinel pellets (*6*), but the activation energy remained constant indicating that the poisoning was geometrical. The data that are available (*5–10*) have many severe limitations that make fundamental interpretation impossible. Steady state was frequently not demonstrated, and in none of the studies was the presence of a dynamic equilibrium between gas and metal surface demonstrated, although this is essential if the results are to be quantitatively interpreted. It is frequently stated that S poisoning is irreversible but such statements have little quantitative value without at least some equilibrium information. No catalytic studies have determined the amount of S adsorbed by the metal. The extreme sensitivity of transition metals to S even under conditions where the bulk metal sulfide is clearly not stable has led to suggestions that S deactivation was due to pronounced electronic effects but other evidence to support this speculation is lacking. Similarly there

[1] Present address: Amoco Oil Co., Naperville, Illinois.

[2] Present address: Central Research Department, Mobil Research and Development Corporation, Princeton, New Jersey 08540. To whom correspondence should be addressed.

[3] Experimental Station, I. E. du Pont de Nemours and Co., Inc., Wilmington, Delaware.

0021-9517/82/080369-16$02.00/0

is no information available on the rates of S deactivation although such data could help greatly in the interpretation of S poisoning.

Many of the problems with the available data arise from the experimental techniques used to obtain them. Sulfur poisoning studies have usually involved fixed-bed reactors and metal catalysts on porous supports. It is impossible to measure intrinsic rates of deactivation with such techniques because a poisoning wave moves slowly through the reactor axially, and a second poisoning wave moves slowly radially into each porous catalyst particle. An a priori model must be fitted to the data to calculate poisoning rates, making fundamental interpretation difficult if not impossible because of model discrimination problems.

The objectives of this study were to measure the rate and extent of S poisoning (H_2S) of Ni catalysts in CO hydrogenation and to develop a fundamental understanding of the mechanism of S poisoning. Experimental techniques (discussed below) were first developed to allow quantitative measurement of the rate and extent of S poisoning, and rates and extents of poisoning by H_2S were determined for 10 to 100 ppb H_2S in the hydrogenation of CO to CH_4. The effects of dispersion and support interactions were assessed by comparing poisoning data on Ni foils and on Ni films on α-Al_2O_3 and SiO_2 with that of Ni supported on α-Al_2O_3.

EXPERIMENTAL METHODS

To allow quantitative determination of rates of S deactivation, of extents of S deactivation at required very low H_2S concentrations, of true dynamic equilibrium between gas and metal surface, and of the amount of S adsorbed, the experimental apparatus and procedure must satisfy the following requirements:

(1) The reactor must be gradientless with respect to reactant and to S concentration so that all parts of the catalyst are exposed to the same gas-phase S concentration. Even a shallow bed of catalyst operated at $<1\%$ CO conversion is not necessarily gradientless with respect to H_2S. Because of the very strong adsorption of S on metals, a poisoning wave moves through even a very shallow catalyst bed.

(2) All surface metal atoms must be exposed to the same gas-phase concentration of H_2S and of reactants. Because of the very strong adsorption of S, metal atoms a short distance back into a pore will not see the same concentration of S as the metal atoms near the pore mouth or on the exterior surface of the catalyst.

(3) The reactor system must neither adsorb nor give up S at H_2S levels as low as 10 ppb, and feed gas containing controlled H_2S concentrations as low as 10 ppb must be reproducibly preparable.

(4) Analytical capabilities to measure S concentrations below 5 ppb and CH_4 below 1 ppm must be on-line.

In no previous study have all, and in most cases none, of these requirements been met.

A continuous-flow stirred-tank reactor (CSTR) was developed for this study because it satisfies the relevant requirements listed above and allows investigation over a broad range of both product and reactant concentrations. Furthermore, poisoning rates can be measured directly, without requiring assumption of a model for poisoning as long as internal diffusion effects are absent in any porous regions of the catalyst. To eliminate the porous diffusion problem catalysts were prepared on nonporous supports or on very thin exterior peripheral regions of porous supports. The CSTR with a volume of 1260 cm^3 was fabricated from quartz to prevent pick-up of S or release of S under reaction conditions and to permit operation at temperatures above 875 K. Details of the design are described elsewhere (*11–13*).

Feed gas to the reactor was usually supplied by a gas cylinder containing 4% CO in UHP H_2, and the feed gas was passed through a bed of activated charcoal at 473

K to remove metal carbonyls. Hydrogen sulfide was supplied by a cylinder containing 0.9 ppm H_2S in UHP H_2. This stream was metered through a flow controller and then split 50/1 by a glass-lined variable splitter valve (Tracor Instruments) to obtain the requisite low concentrations of H_2S. The low flow stream from the splitter was mixed with the reactor feed. The H_2S concentration in the feed gas to the reactor could be varied from 10 ppb to over 100 ppb. All lines beyond the splitter that contacted the H_2S containing gas stream were either Teflon or glass to avoid adsorption of S. The Teflon lines (3.18 mm o.d.) feeding the reactor were sheathed with polyethylene tubing (6.35 mm o.d.), and He was purged through the annular region between these two lines to eliminate O_2 diffusion into the feed gas. Helium and UHP H_2 were also connected to the flow system to permit the reactor to be purged and heated while being purged with He or H_2 (*12*).

Effluents from the reactor were analyzed for O_2, N_2, CO, CO_2, CH_4, and H_2S by gas chromatography utilizing flame ionization, flame photometry, and thermal conductivity detection.

Accurate analysis of the H_2S concentration to a detectability limit of <4 ppb was achieved using a deactivated silica gel column (Tracor Inc., Austin, TX) at 0°C and a Tracor flame photometric detector (FPD). The column and all GC tubing consisted of FEP[19] Teflon, and the gas sample values were Carpenter-20 steel to minimize sulfur pick-up. The FPD utilized quartz flame jets and all glass-lined fittings. Adsorption of the sample was further minimized by passivating the sample loops, column, and FPD by injecting a standard gas (0.9 ppm H_2S in H_2) before analysis of the reactor gases.

Materials

Gases. All of the reactor feed gases were of ultra-high purity. The 4% CO/96% H_2 mixture was certified "primary standard" by Matheson. The H_2S/H_2 mixtures (10.0 and 0.90 ppm H_2S) were prepared, stabilized and analyzed by Matheson.

Catalysts were prepared in our laboratory (*12*) to meet the requirements of all surface metal atoms being exposed to the same gas-phase H_2S concentration. Nickel foil, Ni evaporated onto nonporous SiO_2 and fused α-Al_2O_3, and Ni impregnated onto nonporous fused α-Al_2O_3 and onto porous 6.4-mm α-Al_2O_3 spheres were used as catalysts. The evaporated film catalysts were prepared by vacuum evaporation of carbonyl-refined Ni powder onto a rotating quartz or α-Al_2O_3 cylinder in an oil-free, ion-pumped vacuum system. The Ni surface was passivated by contact with purified O_2 in the vacuum chamber prior to contact with the atmosphere. The impregnated Ni/α-Al_2O_3 catalysts were prepared by dipping fused α-Al_2O_3 plates into a nickel ammonium nitrate solution. The α-alumina plates (Coors Porcelain) had been pretreated at 1273 K, first in flowing H_2 for 8 hr then for a similar period in flowing O_2. After drying, the catalysts, impregnated with Ni, were calcined in flowing O_2 at 623 K. The more disperse impregnated Ni/α-Al_2O_3 spherical pellets were prepared by precipitating the Ni in a thin peripheral region around the outside of the porous spheres (Catalyst and Chemicals α-Al_2O_3, 6.4 mm diameter; BET surface area 1 m^2/g), giving a very thin "egg shell" catalyst containing 0.22 wt% Ni. Catalysts were rapidly blotted, dried, and calcined in O_2 at 623 K. The Ni foils were "MARZ" grade (Ventron Corp.), 0.025 mm thick, and contained initially 0.35 ppm by weight of S, according to the supplier's analysis. Foils were cleaned by repeated cycles of 923 K oxidation followed by 923 K H_2 reduction and were passivated by O_2 at 298 K before contact with the atmosphere. If catalysts were not passivated with O_2, sufficient S was picked up in transfer through the atmosphere to severely reduce initial activity.

Ion sputtering combined with AES applied to the evaporated Ni/quartz films indicated film thicknesses of 500 to 1000 Å.

The catalysts were examined by scanning electron microscopy (SEM) and Auger electron spectroscopy (AES). The crystallites of the fused α-Al_2O_3 were approximately 3.5 μm in dimension, and the Ni surface was electrically continuous as observed by AES and had crystallites of Ni as large as 800–1000 Å across. Calculations based on the quantity of impregnation solution wetting the surface predicted a Ni film thickness of 500 to 1000 Å, in accord with the AES sputtering results.

The surface area of the Ni on the periphery of the Al_2O_3 spheres was 148 cm^2/g catalyst as determined by H_2 chemisorption at 25°C following reduction at 350°C in flowing H_2, and the dispersion was 0.0065. Assuming square Ni crystallites the calculated average dimension was 350 Å. SEM showed that the Ni was located in a peripheral shell about 1 μm thick on the α-Al_2O_3 spheres, which were 0.64 cm in diameter. Hydrogen chemisorption could not be carried out on the Ni catalysts prepared by evaporation or surface impregnation on fused α-Al_2O_3 and SiO_2 (quartz) because of the extremely low Ni surface areas. For these samples, Ni surface areas were estimated by applying a roughness factor of 1.0 to the geometric surface area.

Procedure

The unreduced supported nickel oxide catalysts or surface-passivated Ni films and foils were placed in the reactor. This procedure greatly minimized contamination of the catalyst surface during transfer to the reactor. To further safeguard the catalyst from contamination, all transfers were made directly from the furnace preparation tubes to either the reactor or a gas-tight storage bottle via a nitrogen-purged glove bag. Improper handling resulted in sufficient sulfur adsorption from the atmosphere (30 ppb sulfur compounds) to markedly reduce the initial activity.

With the catalyst sealed in the reactor, He was purged through the CSTR at room temperature to remove all other gases; removal was verified in each experiment by analyzing reactor effluent gas by TC. The reactor was next purged with H_2 and then heated to the desired temperature in flowing H_2. When the desired temperature was reached, the feed mixture of CO, H_2, and H_2S was started, and the activity-time behavior was followed until steady state was reached. Standard operating conditions included 1.1 atm total pressure, 661 K, 4% CO in UHP H_2, and a feed rate of 90–100 cm^3/min; sulfur (H_2S) concentration (0 to 100 ppb) was the main variable. The reaction temperature and feed gas composition were varied to determine the activation energy for methanation and the rate dependence on CO and H_2S concentration for each catalyst.

The S/Ni ratio on steady-state poisoned Ni impregnated fused α-Al_2O_3 plates was measured by AES. After the poisoning study was completed, the catalyst was cooled to 298 K in the reactor. The surface was passivated with a stream of 5% O_2 in He, and the catalyst was transferred to the Auger spectrometer. The sample was heated in H_2 at 10^{-7} Torr to remove the oxide formed during passivation, and the surface was analyzed by AES to determine the nickel (100 eV) to sulfur (151 eV) peak ratio. The surface was then sputtered with A^+ ions to determine the depth of the sulfur-containing layer present.

RESULTS

Sulfur-Free Methanation Kinetics

Kinetic validity. The plate and "egg shell" catalysts used in this study were chosen to be free of internal diffusion effects. Mass-transfer calculations indicated that under the conditions studied the rates of external transport of gaseous species even at concentrations as low as 50 ppb were 1000-fold greater than the rates of surface reaction and that intraparticle mass-transfer limitations were also absent. This, coupled with the excellent mixing in the reactor, ensured that each metal site was

exposed to the same known uniform gas concentration as a function of time. This allowed direct measurement of the rate of poisoning by sulfur and carbon and of the rate of reaction in kinetic studies. Reactor and catalyst transients were not perturbed by mass-transfer effects, and the effluent analyses unequivocally indicated when steady state had been reached. The absence of any mass-transfer effects in a gradientless reactor also permitted direct analysis of the data without assumptions of any kinetic or poisoning models. Except during approximately the first hour of operation the reactor was in essentially steady-state operation. Nevertheless, instantaneous reaction rates were calculated from a transient reactor model based on CH_4 concentration in the reactor effluent. The rates are expressed as turnover numbers, reaction events per surface Ni atom per second.

Initial transient behavior. During the first hour the methanation rate rose sharply from zero to about eight times the final steady-state rate and then declined to the steady-state value. This transient was due to both physical and chemical phenomena. The CO concentration increased from zero to 4.0% over a 40- to 50-min period during the early part of the startup of the H_2-filled reactor; this coupled with the positive order kinetic dependence on CO concentration should have caused the rate to increase asymptotically to the steady-state value in less than 1 hr, which was about four average residence times for the reactor. The eightfold overshoot observed was therefore attributed to transient behavior in the catalytic activity of the Ni, possibly arising from residual oxygen in the catalyst, but this was not studied further.

Fresh Ni/α-Al_2O_3 reached a steady-state rate within less than 60 min and maintained that activity thereafter with only very slow deactivation, less than 10% per 24 hr. The activity loss after several days' operation was totally recoverable by treatment in H_2 at reaction temperature for several hours. From this it was concluded that this slow activity loss was due to carbon build-up on the Ni and not due to background contaminant sulfur.

Methanation kinetics. The variation in the steady-state methanation rate with the CO partial pressure is shown in Fig. 1. Data were obtained by varying the CO concentrations from 0.5 to 4%, then increasing the concentration to 20% CO and repeating consecutively the points at 0.5 and at 20%. The lower methanation rate at the highest CO partial pressures is indicative of competitive adsorption of CO and H_2 and can best be understood on the basis of Langmuir–Hinshelwood kinetics; the line through the data is a best fit Langmuir–Hinshelwood rate expression which will be discussed below. With increasing CO partial pressure more CO adsorbs, reducing the surface available for hydrogen, and thus the methanation rate decreases. The effect of CO partial pressure was reversible and kinetic since decreasing the gas-phase CO concentration from 20 to 0.5% reproduced the rate at the lower CO concentration; return to 20% CO reproduced this rate again also.

Figure 2 shows the temperature dependence of the CO hydrogenation rate for three of the Ni/α-Al_2O_3 catalysts studied.

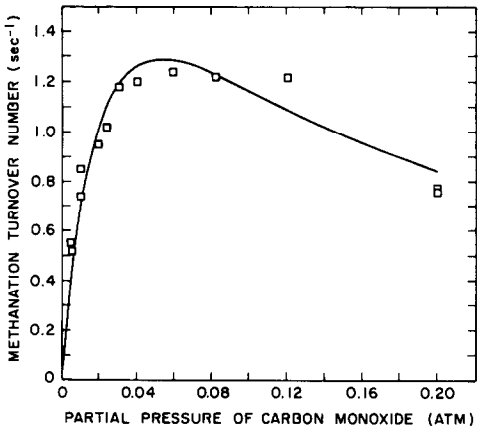

FIG. 1. CO pressure dependence of methanation rate catalyzed by Ni film. Reaction conditions: 661 K, P_{H_2} = 0.88 atm, P_{H_2S} = 0.0. (The indicated curve is a nonlinear least-squares fit.)

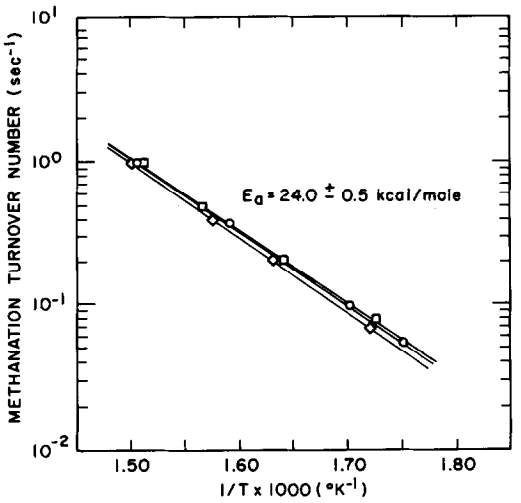

FIG. 2. Temperature dependence of the CO hydrogenation catalyzed by ◇, evaporated Ni/α-Al_2O_3; □, Ni/α-Al_2O_3 (impregnated on fused α-Al_2O_3 plate): ○, Ni/α-Al_2O_3 pellets. Reaction conditions: P_{CO} = 0.044 atm, P_{H_2} = 1.056 atm, P_{H_2S} = 0.0.

Steady-state turnover numbers at standard reaction conditions and activation energies for all catalysts studied are summarized in Table 1. The activation energy of all of the Ni/α-Al_2O_3 catalysts for methanation was 24.0 ± 0.5 kcal/mole, regardless of the catalyst and its preparation procedures.

The Ni/SiO_2 (quartz) gave reproducible activation energies of 18.4 ± 0.2 kcal/mole. With the exception of the support used, all preparation and run conditions were the same for the Ni/α-Al_2O_3 and the Ni/SiO_2 catalysts.

Sulfur Poisoning Studies

Sulfur poisoning studies were carried out by *in situ poisoning* in which CO, H_2, and H_2S were all fed to the reactor at the same time, and the rate of methanation was followed as poisoning occurred during reaction. Sulfur poisoning was also studied by *prepoisoning* in which the Ni/α-Al_2O_3 was first equilibrated with H_2S in H_2 at the reaction temperature, and when adsorption equilibrium for H_2S had been achieved, the feed gas was changed to H_2, CO, and H_2S at the prepoisoning concentration. In all experiments the concentration of CH_4 and of H_2S in the exit gas from the reactor was determined as a function of time. Separate studies with the reactor alone and with the reactor containing the several supports used but without Ni on them showed that neither the reactor nor the support adsorbed measurable quantities of H_2S. The observed H_2S transients were only slightly different from the predicted reactor transient for no H_2S adsorption. At steady state

TABLE 1

Sulfur-Free Steady-State Methanation Kinetics

Catalyst[a]	Method of preparation	Methanation turnover number[b] (s^{-1})	E_a (kcal/mole)
Ni/α-Al_2O_3 (pellets)	Precipitation	1.0	24.0
		1.2	—
Ni/α-Al_2O_3 (fused plate)	Impregnation	0.9	23.5
		1.1	—
Ni/α-Al_2O_3 (fused plate)	Evaporation	1.0	24.3
Ni/SiO_2 (quartz)[c]		0.9	18.3
		1.3	18.5
		1.1	18.0

[a] Multiple entries represent determinations on separate catalysts.

[b] Steady-state rates at standard reaction conditions: 661 K, 4.0% CO in H_2, 1.1 atm total pressure, <1.0 ppb sulfur.

[c] Active surface area was assumed to be the geometric area of the support, i.e., roughness factor = 1.0.

the reactor effluent contained the same H_2S concentration as added to the reactor (*12, 13*). Thus when sulfur adsorption was observed, it was associated solely with the Ni.

Figure 3 shows the decay in the methanation activity of a fused α-Al_2O_3 plate impregnated with Ni, and Fig. 4 shows the corresponding H_2S concentrations in the CSTR as measured by the exit H_2S concentration as a function of time. The presence of just 13 ppb H_2S in the gas phase in the reactor caused more than a 100-fold reduction in methanation activity. In the run shown in Fig. 3 steady-state activity was achieved in about 3500 min, at which point the H_2S concentration was increased from 13 to 62 ppb. Other runs which were carried on for considerably longer times with 13 ppb H_2S in the gas phase demonstrated that the steady-state turnover number was from 0.5×10^{-3} to 0.6×10^{-3} s^{-1}.

Over 3000 min was required to reach steady-state activity for 12 to 15 ppb H_2S in the feed. No H_2S could be detected in the CFSTR effluent for over 1000 min indicating that all H_2S added was adsorbed by the catalyst (Fig. 4). Although the reactor contained only about 30 cm^2 of Ni surface area, a long time was required before the reactor reached steady state with respect to S because of the very low concentrations of H_2S added (13 ppb). About 5000 min is required to feed enough H_2S to add one S atom per surface Ni atom, i.e., the observed rate of deactivation over a major portion of the time was governed by the S addition rate.

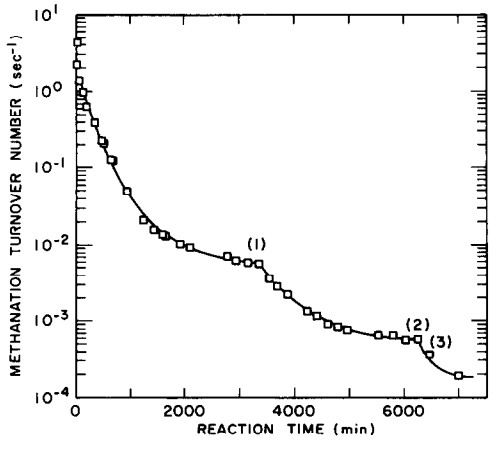

FIG. 3. Sensitivity of the Ni/α-Al_2O_3, impregnated on fused Al_2O_3 plates, to H_2S poisoning. Reaction conditions: CFSTR, 661 K, P_{H_2} = 1.056 atm, P_{CO} = 0.044 atm, P_{H_2S} = 13 ppb from t = 0.0 to point (1); P_{H_2S} = 62 ppb from point (1) to point (2); P_{H_2S} = 95 ppb from point (2) to point (3).

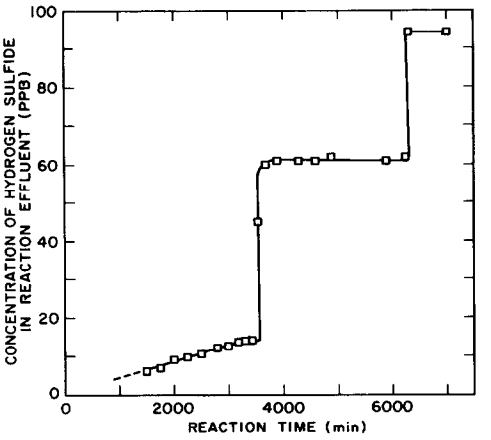

FIG. 4. Transients in the H_2S concentration in the reactor exit observed during the S poisoning of the Ni/α-Al_2O_3 (impregnated on fused α-Al_2O_3 plates). Reaction conditions: 661 K, P_{H_2} = 1.056 atm, P_{CO} = 0.044 atm, P_{H_2S} = 13 ppb in feed from t = 0 to 3500 min; P_{H_2S} = 62 ppb from 3500 to 6500 min, P_{H_2S} = 95 ppb beyond 6500 min.

AES analysis of Ni films which had been poisoned to steady-state CO hydrogenation activity in the presence of 13 ppb H_2S, passivated, transferred to the spectrometer, reduced in H_2 (10^{-7} Torr), and analyzed gave a S (151 eV) to Ni (100 eV) peak height ratio of 1.2 to 1.0; this ratio is representative of a monolayer of S on Ni which should be about 0.5 to 0.6 S atoms per surface Ni atom (*14–19*). The S/Ni peak ratio of bulk NiS is 4.0 (*19*). When the surface was sputtered with A^+ ions, the S signal went to zero in approximately the time required to sputter away one monolayer. Clearly the equilibrium Ni surface for 13 ppb H_2S in H_2 contained essentially a monolayer of S atoms and no more under conditions in which no bulk nickel sulfide was thermodynamically stable.

Increasing the H_2S concentration to 62 ppb resulted in an additional 10-fold reduction in methanation activity; an increase to 95 ppb H_2S reduced the activity more than fivefold further (Fig. 3). Comparing the methanation rates, in Fig. 3 with the H_2S concentration transients in Fig. 4 indicates that for the prolonged adsorption of H_2S during the 13 ppb deactivation the H_2S level reached a steady state at about the same time as the methanation rate. Figure 4 shows that increasing the H_2S level stepwise above 13 ppb resulted in little further pickup of H_2S by the Ni, although the methanation activity continued to decline for periods of time markedly beyond that required for the exit S level to equal that added (Fig. 3). Careful examination of the results indicated that small but difficult to quantify amounts of S were adsorbed.

Several other experiments not only exhibited deactivation similar to that in Fig. 3 but also showed that the steady-state activity of the catalyst depends on the steady-state gas-phase H_2S concentration and is independent of the prior H_2S concentration history. Another Ni/α-Al_2O_3 (impregnated fused plate) catalyst was deactivated in a constant 55 ppb H_2S to a steady-state activity of 6×10^{-4} s^{-1}, which is the same as that observed for the 62 ppb H_2S steady state for the impregnated plate catalyst in Fig. 3.

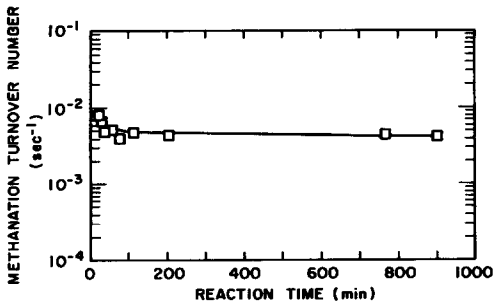

FIG. 5. Methanation transient observed after presulfiding and equilibrating Ni/α-Al_2O_3 (impregnated on fused plate) for 50 hr using 13 ppb H_2S in H_2; T = 661 K, P_{H_2S} = 13 ppb at steady state; 50 hr with 13 ppb H_2S in H_2 at 661 K, then switching to a standard reaction feed of 4% CO in H_2, 661 K; 15 ppb H_2S, 1.1 atm.

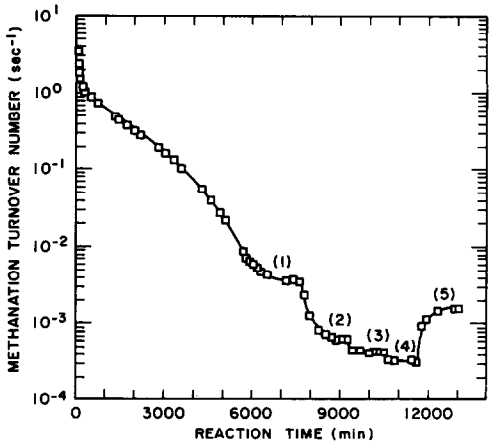

FIG. 6. Sensitivity of the "egg shell" Ni/α-Al_2O_3 sphere catalyst to H_2S poisoning. Reaction conditions: CFSTR, 661 K, P_{H_2} = 1.056 atm, P_{CO} = 0.044 atm, P_{H_2S} = 12 ppb from t = 0 to point (1); P_{H_2S} = 52 ppb from point (1) to point (2); P_{H_2S} = 73 ppb from point (2) to point (3); P_{H_2S} = 93 ppb from point (3) to point (4); P_{H_2S} = 15 ppb from point (4) to point (5).

When an impregnated fused plate Ni/α-Al_2O_3 catalyst was first equilibrated with 13 ppb H_2S in H_2 at 661 K in the absence of CO (prepoisoned) and then the reactor feed was switched to 4% CO and 15 ppb H_2S in H_2, steady state was reached at the end of the 1-hr purge period (Fig. 5). The observed turnover number of 5×10^{-3} s^{-1} for *prepoisoning* is very close to that for *in situ* poisoning, 6×10^{-3} s^{-1} with 13 ppb H_2S in CO plus H_2 (Fig. 3).

Deactivation behavior of the "egg shell" Ni/α-Al_2O_3 sphere catalyst (Fig. 6) is similar to that of the impregnated and evaporated film plate catalysts. In another experiment this catalyst was deactivated at a constant 55 ppb H_2S to a steady-state activity of 6×10^{-4} s^{-1}, which is the same as that for 62 ppb H_2S in Fig. 3. In another part of the run shown in Fig. 6, the H_2S level in the reactor was decreased from 93 to 15 ppb, and an increase in the methanation rate was observed. In addition to indicating that the rates observed represent steady-state rates, the data uniquely show that the S adsorption and deactivation are reversible. The steady-state methanation rate for *in situ*

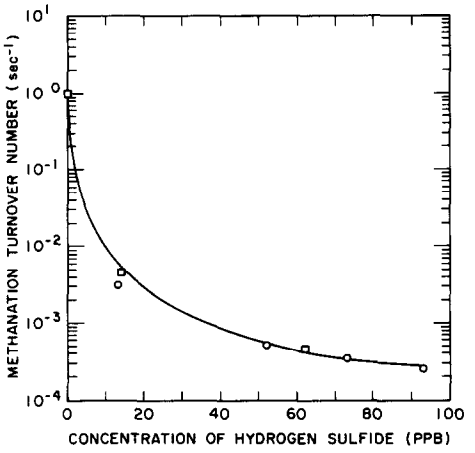

FIG. 7. Dependence of the steady-state equilibrium S poisoned Ni methanation rate on the gas-phase H_2S concentration. Reaction conditions: CFSTR, 661 K, $P_{H_2} = 1.056$ atm, $P_{CO} = 0.044$ atm; ○, Ni impregnated on fused α-Al_2O_3 catalyst; □, "egg shell" Ni/α-Al_2O_3 catalyst.

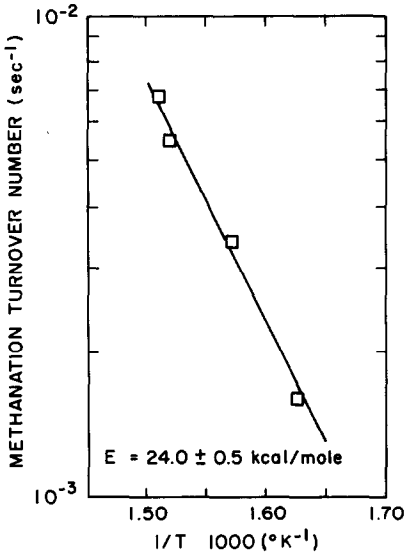

FIG. 8. Temperature dependence of the CO hydrogenation rate over equilibrium sulfided Ni/α-Al_2O_3, 4% CO, 96% H_2, $P_{H_2S} = 13$ ppb at steady state, Ni/Al_2O_3. Reaction conditions: Ni impregnated on fused α-Al_2O_3, CFSTR, $P_{H_2} = 1.056$ atm, $P_{CO} = 0.044$ atm, $P_{H_2S} = 13$ ppb.

poisoning of 13 ppb H_2S was 4×10^{-3} s^{-1}, and the rate for 15 ppb H_2S after recovery for 500 min was about 2×10^{-3} s^{-1} indicating essentially complete reversibility of S poisoning and little deactivation from C deposition. To the best of our knowledge this is the first time that reversibility in S poisoning has been demonstrated. These results show that S poisoning should be *totally* reversible.

Figure 7, which shows steady-state equilibrium poisoned rates for the impregnated and precipitated catalysts as a function of gas-phase H_2S concentration, summarizes the steady-state rate information generated. Figure 8 shows the temperature dependence of the CO hydrogenation rate for the impregnated fused α-Al_2O_3 plate catalyst with 13 ppb H_2S in the gas phase. The activation energy, 24.0 ± 0.5 kcal, is the same as with the un-sulfur-poisoned catalysts (Table 1, Fig. 2).

The results of a high spot study of the sulfur poisoning of a cleaned Ni foil is summarized in Fig. 9. The foil reached an apparent steady-state methanation rate of 6×10^{-4} s^{-1} which is lower than that measured for the Ni/α-Al_2O_3 catalysts at comparable H_2S levels. Much of the difference is attributed to initial contamination of the foil, which was very hard to clean; many cleaning techniques were tried giving variable initial foil activity. The assumptions of roughness factors used in calculating the Ni surface area of the foil and of the Ni on the fused plates may contribute to some of the differences. We speculate that S diffusing from the bulk of the polycrystalline Ni foil

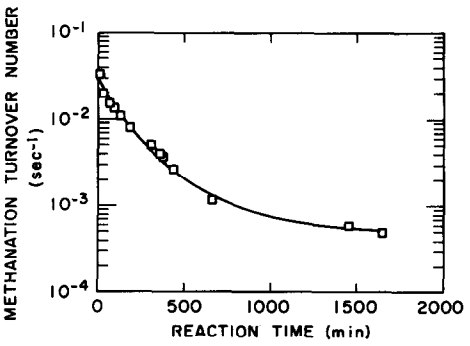

FIG. 9. Sulfur deactivation of a Ni foil; reaction conditions: CFSTR, 661 K, $P_{H_2} = 1.056$ atm, $P_{CO} = 0.044$ atm, $P_{H_2S} = 13$ ppb.

may have resulted in a significant increase in surface S concentration, and that this accounts for most of the apparent difference in intrinsic activity.

DISCUSSION

Effect of Sulfur Adsorption on Nickel Surfaces

Figures 3 and 4 show that the Ni surface has become equilibrated with S from 13 ppb H_2S in H_2 plus CO within 3500 min. AES studies strongly suggested that the amount of S present was essentially a monolayer on the Ni surface and that the S atom to surface Ni atom ratio was about 0.6 to 1.0. To further quantify the amount of S present and hence the extent of coverage of the Ni by S the amount of S was determined from a material balance around the reactor which integrated over time gave the total amount of S adsorbed between any two times, including between zero time and equilibrium. Since experiments showed that the reactor and the catalyst supports did not adsorb S, i.e., the H_2S transient without Ni present was that predicted by a physical model for the system, all S which disappeared was adsorbed on the Ni surface. For the Ni/α-Al_2O_3 spheres the chemisorption measure of the number of surface Ni atoms was 3.1×10^{-7} gatom Ni/g cat (1.6×10^{-7} gmol H_2/g cat); the total amount of S adsorbed, as determined by integrating the S material balance about the CFSTR from zero time to steady state, for 13 ppb H_2S in H_2 plus CO at 661 K was 1.6×10^{-7} gatoms S/g cat. Table 2 summarizes the results for several experiments in terms of the amount of catalyst in the reactor using 1 to 1 and 0.5 to 1 adsorbed atom to surface Ni atom stoichiometry for hydrogen and S adsorption, respectively. For the Ni-impregnated α-Al_2O_3 plates the surface area was estimated from the geometric surface area and a roughness factor of 1.0 because accurate chemisorption was not possible. The S adsorption measurements give a good correspondence with the expected Ni surface area; the area variations observed are probably real as plate size varied.

TABLE 2

Surface Area of Ni Catalysts from Hydrogen and Sulfur Adsorption

Catalyst	Hydrogen chemisorption area[a] (cm^2)	Sulfur adsorption area[b] (cm^2)
Ni/α-Al_2O_3	300	300
(spheres)	300	310
Ni/α-Al_2O_3	75[c]	60
(flat plates)		100
		80

[a] Calculated assuming 1 to 1 H atom to surface Ni atom stoichiometry and an effective area of 6.3×10^{-16} cm^2 per atom.

[b] Calculated assuming a 0.5 to 1 S atom to surface Ni atom stoichiometry and an effective area of 6.3×10^{-16} cm^2 per atom.

[c] Approximated from geometric area of the flat plate using a roughness factor of 1.0.

These results clearly show that the formation of a surface monolayer of S on Ni and that this monolayer has a stoichiometry of about one S atom per two surface Ni atoms. This is in accord with the AES results and clearly shows the formation of a stable surface sulfide phase under conditions which are very far from those required to form any stable bulk nickel sulfide phases.

Saturation at this low level leads to the prediction that the free energy of formation of the two-dimensional surface sulfide at 661 K is at least -26 kcal/mole. Compared with ΔG_f of -11 kcal/mole for the formation of bulk Ni_2S_3 at the same temperature, the two-dimensional surface sulfide is 15 kcal/mole more stable than the most stable bulk nickel sulfide.

The number of adsorbed S atoms as a function of time can be calculated from the area between the measured H_2S transient curve and the feed H_2S concentration up to that time and the fraction of a S monolayer as a function of time is that area divided by the total area obtained from steady state.

The measured rate data in the submonolayer region of Fig. 3 can be combined with the S coverage data to yield a nonlinear relationship between the turnover number and the fraction of the surface poisoned by S. Figure 10 shows that the rate varies with the square of the unpoisoned fraction of the surface. In the case of these data, this relationship is kinetically significant and not coincidental because all of the surface Ni atoms are uniformly exposed to a uniform gas-phase composition of all species, including H_2S. This means that the Ni surface is undergoing uniform S poisoning, and the observed rate is a fundamental quantity for the uniformly S-poisoned surface containing the measured amount of S. If the S adsorption had been in the form of surface islands of adsorbed S, the rate would have been expected to be reduced in a linear manner with the amount of unpoisoned surface as it is when activity reduction is due to a poisoning wave moving through a catalyst bed. The fact that activity reduction is nonlinear in surface S coverage strongly suggests that the S is uniformly distributed across and randomly located on the surface; island formation does not occur under these conditions (*20*). The mechanism of S poisoning of CO hydrogenation by S blockage will be discussed below.

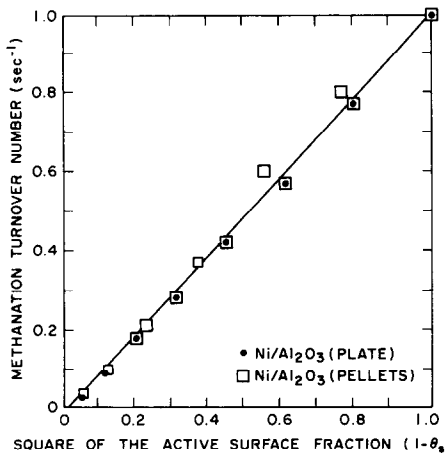

FIG. 10. Variation in methanation rate of Ni/α-Al_2O_3 with the square of the unpoisoned surface fraction. Reaction conditions: CFSTR, 661 K, P_{H_2} = 1.056 atm, P_{CO} = 0.044 atm, P_{H_2S} = 55 ppb; ●, Ni impregnated fused α-Al_2O_3 plates; □, "egg shell" Ni/α-Al_2O_3 spheres.

The development so far fails to account for the further decrease in methanation activity when the H_2S level is increased above 15 ppb. Additional information is obtained by making the reasonable assumption that H_2S adsorption can be represented by a Langmuir adsorption isotherm (*14, 21*). Thus, when the CO hydrogenation activity is reduced 200-fold by 13 ppb H_2S, we infer that a very few active CO hydrogenation sites remain and that these are progressively removed by adsorption of S at higher H_2S concentrations. The kinetic implications of this are considered below.

Mechanism of Sulfur Poisoning

Activation energy. Figures 2 and 8 show that the activation energy for methanation is the same (24.0 ± 0.5 kcal/mole) for a S poisoned and an unpoisoned Ni/α-Al_2O_3 catalyst (Table 1). This invariance of the activation energy with S poisoning and the marked (>100-fold) catalyst activity reduction indicates that S poisoning is due to a geometric blockage mechanism. The adsorbed S atoms appear to block active Ni surface sites without energetically affecting neighboring Ni sites. If S poisoning had been due to electronic effects, these effects should have appeared as a change in the activation energy for CO hydrogenation catalyzed by the sulfur-poisoned Ni/α-Al_2O_3; this was not observed. Similar phenomena have been observed by Ponec and coworkers (*22, 23*) in studies of methanation over Ni/Cu films where Cu segregated preferentially to the surface and caused severe reductions in the rate of CO hydrogenation without changing the activation energy for methanation as compared to that for pure Ni films. Ponec attributed this result to the fact that Cu atoms occupied those ensemble sites which were active for CO dissociation and reduced the rate by purely geometric means. He further argued that Cu blocked these sites where back-donation of elec-

trons is sufficient to dissociate CO (bridged sites), preventing dissociation of CO and hence preventing methanation.

Further evidence to support the argument that S blocks Ni in much the same manner as does Cu comes from infrared studies of the effects of S adsorption on the adsorption of CO on Ni (*24*) which demonstrated that the addition of S to Ni eliminates the bridge-bound or high coordination CO species. However, the presence of the linear CO species, a low coordination species, is unaffected by the presence of S. Similarly, Kishi and Roberts (*25*) using UPS found that as S was adsorbed on Fe the surface lost its ability to bond the bridged CO species. They concluded that the sites occupied by S were exactly those sites necessary for CO dissociation. These spectroscopic studies further support the contention that S poisons the methanation activity of metal catalysts through a geometric or site blockage mechanism, in this case blocking those sites of multiple coordination which are responsible for CO dissociation. No study has concluded that S adsorption changes the bonding of CO to Ni, reducing the rate of or eliminating CO dissociation and thus poisoning methanation; all studies have concluded that S (or Cu) eliminates or blocks specific sites on the surface and thus blocks reaction, a geometric effect. By preventing CO dissociation, the S atoms effectively poison the reaction at the surface carbon-formation step

$$CO_{(ad)} \rightarrow C_{(ad)} + O_{(ad)}$$

CO hydrogenation kinetics. Reaction kinetics can be treated purely empirically by fitting a range of Langmuir–Hinshelwood or power-law type models until an adequate fit is achieved; we prefer to derive appropriate kinetic models using all available chemical information and then to fit these to the observed rate behavior. This should provide relevant additional insight and interpretation of the behavior observed keeping in mind that kinetic results are never definitive.

The rate behavior will be discussed on the basis of two kinetic models which assume that the reaction involves CO dissociation (*11, 22–30*) and that the rate-determining step in the reaction sequence requires two Ni sites. The first mechanism assumes that the dissociation of adsorbed CO molecules is the rate-determining step in the reaction sequence; the second assumes that the rate-determining step is the reaction between adsorbed C and H atoms on the surface. Both mechanisms assume that CH_4 formation results from the hydrogenation of a surface "carbidic" species on the Ni surface rather than of an oxygen-containing species. The predictions of each model will be examined and compared with the observed dependence of the rate on the CO partial pressure (Fig. 1) and on the fraction of unpoisoned sites (Fig. 10). The elementary reaction steps considered are:

$$H_{2(g)} \rightleftarrows 2H_{(ad)} \quad (1)$$

$$CO_{(g)} \rightleftarrows CO_{(ad)} \quad (2)$$

$$CO_{(ad)} \xrightarrow{k_1} C_{(ad)} + O_{(ad)} \quad (3)$$

$$C_{(ad)} + H_{(ad)} \xrightarrow{k_2} CH_{(ad)} \quad (4)$$

$$CH_{(ad)} + H_{(ad)} \xrightarrow{k_3} CH_{2(ad)} \quad (5)$$

$$CH_{2(ad)} + 2H_{(ad)} \xrightarrow{k_4} CH_{4(ad)} \quad (6)$$

$$O_{(ad)} + 2H_{(ad)} \xrightarrow{k_5} HOH_{(ad)} \quad (7)$$

$$H_2O_{(ad)} \rightarrow H_2O_{(g)} \quad (8)$$

$$CH_{4(ad)} \rightarrow CH_{4(g)} \quad (9)$$

Steps occurring after the rate-determining step are not kinetically important, and are therefore expressed in an abbreviated manner.

Therefore, for Model I [CO dissociation is rate limiting]:

$$r = k\,\theta_{CO}\theta_V \quad (10)$$

where θ_{CO} is the fraction of surface sites

covered by adsorbed CO, and θ_V is the fraction of surface sites which are vacant.

Defining X as the fraction of surface sites which do not have sulfur adsorbed on them,

$$X = 1 - \theta_S = \theta_V + \theta_{CO} + \theta_H + \theta_O + \theta_C + \theta_{H_2O} + \theta_{CH_4} + \ldots \quad (11)$$

Carrying out the standard kinetic analysis for the CO hydrogenation based on the above definitions (*31–33*) and simplifying the expression in terms of constants and variable terms gives (*12*):

$$r = \frac{K_1 P_{CO} X^2}{(K_2 + K_3 P_{CO})^2}. \quad (12)$$

For Model II [hydrogenation of adsorbed carbon species is rate determining] kinetic analysis gives (*12*):

$$r = \frac{K_1' P_{H_2}^{1/2} P_{CO} X^2}{(K_2' + K_3' P_{CO})^2}. \quad (13)$$

The kinetic expressions cannot be distinguished without H_2 partial pressure dependence, not available here. Schoube (*34*) and Agrawal (*13, 35*) showed that the rate of methanation followed half-order dependence on H_2 partial pressure for Ni/Al_2O_3 and Co/Al_2O_3, respectively, supporting Eq. (13). Araki and Ponec (*23*) and Wentrcek *et al.* (*27*) conclude that CO dissociation is rate determining; we favor the former conclusion, but further work is needed. A least-squares fit to the data in Fig. 2, with $X = 1.0$ and P_{H_2} constant, gives the equation:

$$r = \frac{91.8\, P_{CO}}{(1 + 17.6\, P_{CO})^2} \quad (14)$$

where r in s^{-1} is the rate expressed as turnover number; P_{CO} is in atm.

The data are fitted well by Eq. (14) (Fig. 2). Further, the models, Eqs. (12) and (13), both predict that the observed rate should depend on the square of the unpoisoned surface fraction, X^2, exactly as observed (Fig. 10), strongly supporting the hypothesis that the rate-determining step in methanation requires two sites. Both the rate behavior in the absence of S poisoning and the kinetic effect of S poisoning support the two site model. The success of the model in predicting S poisoning behavior further supports the conclusion that S poisoning is due to a geometric surface blockage mechanism rather than an electronic effect. The results also indicate that each S atom adsorbs on and eliminates one surface site.

Langmuir adsorption behavior of H_2S. The two-site model for methanation can be utilized to more fully interpret the poisoning results discussed above and to model the dependence of the rate on H_2S partial pressure. Starting with rate Eqs. (12) or (13), X can be expressed in terms of the H_2S partial pressure using a Langmuir isotherm for H_2S adsorption (*26, 35*). From $X = 1 - \theta_S$ and

$$\theta_s = \frac{bP_{H_2S}}{1 + bP_{H_2S}}. \quad (15)$$

Equation (12) becomes

$$r = \frac{K_1 P_{CO}}{(K_2 + K_3 P_{CO})^2} \cdot \frac{1}{(1 + bP_{H_2S})^2}. \quad (16)$$

Equation (13) is similarly transformed. Since the H_2 and CO partial pressure were kept the same in the poisoning experiments, Eq. (15) can be transformed to an expression linear in P_{H_2S}:

$$K/r^{1/2} = 1 + bP_{H_2S} \quad (17)$$

where K = the square root of the methanation rate for unpoisoned catalyst
r = the steady-state methanation rate at a given P_{H_2S}
b = adsorption constant
P_{H_2S} = partial pressure of H_2S in pbb.

Figure 11 shows a plot of the data as per Eq. (16) for Ni-impregnated fused α-Al_2O_3 plates. There are two linear regions present which suggest that Langmuir adsorption behavior holds and that there are two active sites involved. One is very active but strongly adsorbs S and is effectively eliminated by very low H_2S partial pressures; the other is less active and adsorbs S much less

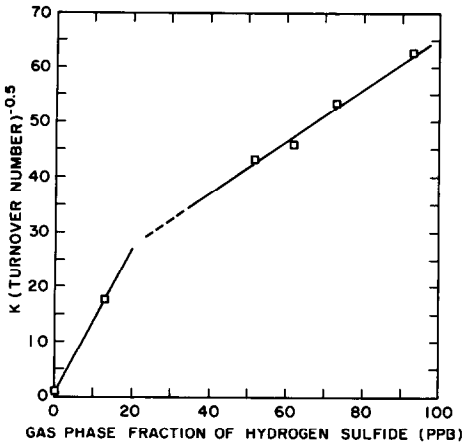

FIG. 11. Dependence of the methanation rate catalyzed by Ni/α-Al_2O_3 on H_2S partial pressure plotted as per Eq. (17). Reaction conditions: CFSTR, Ni impregnated fused α-Al_2O_3 plates, 661 K, P_{H_2} = 1.056 atm, P_{CO} = 0.044 atm.

strongly. From Fig. 11 the more active sites are over 200-fold more active than the less active sites. From the slope of the lines (Fig. 11) the one set of sites adsorbs S almost three times more strongly than the other. A similar conclusion has been reached for the S poisoning of CO hydrogenation catalyzed by Ni/TiO_2 (*36*).

CONCLUSIONS

This work produces a number of important conclusions which provide unique insight into the S poisoning of metals. In order to be able to derive these conclusions an experimental procedure was developed that exposed all surface Ni atoms to a uniform gas-phase composition of all species including H_2S; no gradients existed in the system making kinetic measurements fundamentally meaningful and interpretable. Sulfur poisoning was shown to be reversible, demonstrating that true equilibrium existed between the gas phase and the surface allowing conclusions to be drawn concerning equilibrium behavior. Important conclusions include:

(1) Ni is extremely sensitive to poisoning by S. Concentrations of H_2S as low as 13 ppb in H_2 reduce the steady-state methanation activity of Ni/α-Al_2O_3 catalysts by more than two orders of magnitude. Higher H_2S concentrations further reduce the methanation activity; the activity is reduced 5000-fold by 100 ppb H_2S.

(2) The activation energy for methanation over unpoisoned Ni/α-Al_2O_3 is 24.0 kcal/mole; it is the same for Ni/α-Al_2O_3 in equilibrium with or poisoned by 13 ppb H_2S and having an activity reduced by over 100-fold. This clearly indicates that the S poisoning is due to geometric and not electronic effects.

(3) Concentrations of H_2S as low as 13 ppb in H_2 result in monolayer coverages of Ni by S at 661 K as shown by AES; chemisorption studies show that Ni/Al_2O_3 chemisorbs as many H_2S molecules as H_2 molecules, yielding a S : Ni surface atom stoichiometry of 1 : 2. This is the same S : Ni surface atom ratio found for S adsorption on Ni single crystal surfaces. Sulfur poisoning of Ni methanation catalysts is due to geometric blockage with each S atom capable of blocking one surface Ni site. There is no evidence that poisoning is due to electronic factors since those sites remaining active or unpoisoned appear to be energetically the same as on a S-free surface.

(4) The observed dependence of the methanation rate on the fraction of unpoisoned sites (X) and on the CO partial pressure (P_{CO}) is that predicted by a Langmuir–Hinshelwood analysis of the surface reactions occurring in methanation catalyzed by Ni with either CO dissociation or hydrogenation of surface carbide as rate-determining steps. The rate equation fitted to rate vs P_{CO} data for the Ni/α-Al_2O_3 at 661 K by nonlinear least-squares analysis is:

$$r = \frac{91.8 P_{CO} X^2}{(1 + 17.6 P_{CO})^2}.$$

(5) The free energy of formation of the two-dimensional surface nickel sulfide at 661 K is estimated to be −26 kcal/mole. This is in contrast to the free energy of formation of bulk Ni_2S_3 which is about −11 kcal/mole at this same temperature. The

surface sulfide is therefore at least 15 kcal/mole more stable than the bulk sulfide.

This study shows that the extreme sensitivity of metals to sulfur poisoning is due to the very high thermodynamic stability of surface metal sulfide phases; two-dimensional phases, as contrasted with bulk sulfide phases; bulk thermodynamics cannot be easily used to predict sulfur poisoning. The extensive deactivation is due to geometric effects with S blocking active sites on the surface; there is no evidence for electronic effects in S poisoning of Ni.

APPENDIX 1: NOMENCLATURE

- b Langmuir adsorption constant, atm^{-1}
- C Gas-phase concentration, gmole/cm^3
- E_a Reaction activation energy, kcal/mole
- k Reaction rate constant, s^{-1}
- K_i, K'_i Combination of kinetic constants and adsorption coefficient for adsorbed species on catalyst surface in Langmuir–Hinshelwood kinetic expression, dimensions defined by equations
- K Square root of methanation rate of unpoisoned catalyst, $sec^{1/2}$
- P_i Partial pressure of species i in the gas phase, atm, except for H_2S where units used are ppb
- r Methanation reaction rate, s^{-1}
- t Time, s
- T Temperature, K
- V Reactor volume, cm^3
- X Surface fraction of sites not occupied by sulfur, dimensionless
- θ_i Surface fraction of species i, dimensionless
- θ_V Surface fraction of vacant sites, dimensionless

ACKNOWLEDGMENTS

The financial support of this work by the U.S. DOE Division of Basic Energy Sciences under Contract No. E(11-1)-2579 is greatly appreciated.

REFERENCES

1. Rostrup-Nielson, J. R., *J. Catal.* **11,** 220 (1968).
2. Richardson, J. T., *J. Catal.* **21,** 130 (1971).
3. Rostrup-Nielson, J. R., *J. Catal.* **21,** 171 (1971).
4. Dalla Betta, R. A., Piken, A. G., and Shelef, M., *J. Catal.* **40,** 173 (1975).
5. Cusumano, J. A., Dalla Betta, R. A., and Levy, R. B., Tech. Report to ERDA, No. 2017, Oct., 1976.
6. Rostrup-Nielson, J. R., and Pedersen, K., *J. Catal.* **59,** 395 (1979).
7. Dalla Betta, R. A., and Shelef, M., *Preprints, ACS Div. of Fuel Chem.* **21,** 43 (1976).
8. Fontaine, R., Ph.D. dissertation, Cornell University (1973).
9. Bartholomew, C. H., Final Report to DOE, FE-1790-9, Sept. 6, 1977; Annual Technical Progress Report to DOE, FE-2729-4, Oct. 5, 1978.
10. Bartholomew, C. H., Weatherbee, G. D., and Jarvi, G. A., *J. Catal.* **60,** 257 (1979).
11. Fitzharris, W. D., and Katzer, J. R., *Ind. Eng. Chem. Fund.* **17,** 130 (1978).
12. Fitzharris, W. D., Ph.D. dissertation, University of Delaware (1978).
13. Agrawal, P. K., Ph.D. dissertation, University of Delaware (1979).
14. Fischer, T. E., and Keleman, S. R., *Surface Sci.* **69,** 1 (1977).
15. Bonzel, H. P., and Ku, R., *J. Chem. Phys.* **58,** 4617 (1973).
16. Holloway, P. H., and Hudson, J. B., *Surface Sci.* **33,** 56 (1972).
17. Chang, C. C., *Surface Sci.* **48,** 9 (1975).
18. Colby, S. A., M.Ch.E. dissertation, University of Delaware (1977).
19. McCarroll, J. J., *Surface Sci.* **53,** 297 (1975).
20. Edmonds, T., McCarroll, J. J., and Pitketkley, R. C., *J. Vac. Sci. Tech.* **8,** 68 (1969).
21. DeBoer, J. H., "The Dynamical Character of Adsorption," p. 58. Oxford University Press, 1968.
22. Ponec, V., *Cat. Rev. Sci.-Eng.* **11,** 41 (1975).
23. Araki, M., and Ponec, V., *J. Catal.* **44,** 439 (1976).
24. Rewich, R. T., and Wise, H., *J. Phys. Chem.* **82,** 751 (1978).
25. Kishi, K., and Roberts, M. W., *J. Chem. Soc. Far. Trans. I* **71,** 1715 (1975).
26. Blyholder, G., and Neff, L., *J. Catal.* **2,** 138 (1963).
27. Wentrcek, P. R., Rewick, R. T., and Wise, H., *Fuels* **53,** 274 (1974).
28. Wentrcek, P. R., Wood, B. J., and Wise, H., *J. Catal.* **43,** 363 (1976).
29. Wood, J., and Wise, H., *J. Phys. Chem.* **73,** 1348 (1969).
30. Biloen, P., and Sachtler, W. M. H., *Adv. Catal.* **30,** in press.
31. Smith, J. M., "Chemical Engineering Kinetics." McGraw-Hill, New York, 1970.

32. Carberry, J. J., "Chemical and Catalytic Reaction Engineering." McGraw-Hill, New York, 1976.
33. Froment, G. F., and Bischoff, K. B., "Chemical Reactor Analysis and Design." John Wiley, New York, 1979.
34. Schoubye, P., *J. Catal.* **14,** 238 (1969).
35. Agrawal, P. K., Katzer, J. R., and Manogue, W. H., *Ind. Eng. Chem. Fund.,* submitted (1981).
36. Rao, S. G., M.S. thesis in Chemical Engineering, University of Delaware (1981).